

Spectroscopy of the helium-rich binary ES Ceti reveals accretion via a disc and evidence for eclipses

K. Bąkowska¹, T. R. Marsh², D. Steeghs², G. Nelemans^{3,4,5}, and P. J. Groot^{3,6,7,8}

¹ Institute of Astronomy, Faculty of Physics, Astronomy and Informatics, Nicolaus Copernicus University, ul. Grudziądzka 5, 87-100 Toruń, Poland
e-mail: bakowska@umk.pl

² Department of Physics, University of Warwick, Coventry CV4 7AL, United Kingdom

³ Department of Astrophysics/IMAPP, Radboud University, P O Box 9010, NL-6500 GL Nijmegen, The Netherlands

⁴ Institute of Astronomy, KU Leuven, Celestijnenlaan 200D, B-3001 Leuven, Belgium

⁵ SRON, Netherlands Institute for Space Research, Sorbonnelaan 2, NL-3584 CA Utrecht, The Netherlands

⁶ Department of Astronomy, University of Cape Town, Private Bag X3, Rondebosch, 7701, South Africa

⁷ South African Astronomical Observatory, P.O. Box 9, Observatory, 7935, South Africa

⁸ The Inter-University Institute for Data Intensive Astronomy, University of Cape Town, Private Bag X3, Rondebosch, 7701, South Africa

Received: XXX; accepted: YYY

ABSTRACT

Context. Amongst the hydrogen-deficient accreting binaries known as the "AM CVn stars" are three systems with the shortest known orbital periods: HM Cnc (321 s), V407 Vul (569 s) and ES Cet (620 s). These compact binaries are predicted to be strong sources of persistent gravitational wave radiation. HM Cnc and V407 Vul are undergoing direct impact accretion in which matter transferred from their donor hits the accreting white dwarfs directly. ES Cet, is the longest period of the three and is amongst the most luminous AM CVn stars, but it is not known whether it accretes via a disk or direct impact. ES Cet displays strong HeII 4686 line emission, which is sometimes a sign of magnetically-controlled accretion. Peculiarly, although around one third of hydrogen accreting white dwarfs show evidence for magnetism, none have been found amongst helium accretors.

Aims. We present the results of Magellan and VLT spectroscopic and spectropolarimetric observing campaigns dedicated to ES Cet with the aim of understanding its accretion structure.

Methods. Based on the data collected, we derived trailed spectra, computed Doppler maps of the emission lines, and looked for circular polarisation and variability.

Results. We find strong variability in our spectra on the 620 s period. The lines show evidence for double-peaked emission, characteristic for an accretion disc, with an additional component associated with the outermost disc, rather than a direct impact, that is broadly consistent with "S"-wave emission from the gas stream/disc impact region. This confirms beyond any doubt that 620 s is the orbital period of ES Cet. We find no significant circular polarisation (below 0.1 %). The trailed spectra show that ES Cet's outer disc is eclipsed by the mass donor, revealing at the same time that the photometric minimum coincides with the hitherto unrecognised eclipse.

Conclusions. ES Cet shows spectroscopic behaviour consistent with accretion via a disc, and is the shortest orbital period eclipsing AM CVn star known.

Key words. binaries: close, stars: white dwarfs, cataclysmic variables, individual: ES Ceti

1. Introduction

AM CVn stars are ultra-compact binary systems with orbital periods of 5-65 minutes in which white dwarfs accrete from degenerate or semi-degenerate companions (recent reviews in Solheim 2010; Ramsay et al. 2018). Only hydrogen-deficient material can attain the density necessary to fit within Roche lobes at such short orbital periods and the spectra of AM CVn stars are devoid of hydrogen lines, and are dominated instead by helium, sometimes along with heavier elements (see Warner 1995 for a detailed review).

AM CVn stars and cataclysmic variables (CVs) share many common features, including accretion discs which undergo semi-regular cycles of outburst and quiescence in some cases, and features characteristic of these discs are seen in the spectra of both classes. There are also differences between the two

types; obviously their abundances and orbital periods are very different, but two other distinctions can be drawn. As yet there are no known examples of magnetic white dwarfs amongst almost 60 known AM CVn stars whereas around one third of CVs are magnetic (Pala et al. 2020); there is no obvious explanation for this difference. The other difference is that AM CVn stars can reach such short periods that a novel form of accretion becomes possible in which no accretion disc forms but matter directly impacts the accreting white dwarf instead (Marsh & Steeghs 2002; Marsh, Nelemans & Steeghs 2004).

For decades following the recognition of the nature of AM CVn itself (Smak 1967), only a few members of the class were identified. Even by the year 2000, just six systems were known, but wide-field spectroscopic and photometric surveys have since had a significant impact. By the time of Solheim (2010) 25 systems were known, while 57 were listed

by Ramsay et al. (2018). Because of their short orbital periods, the evolution of AM CVn stars is expected to be governed by gravitational-wave radiation (Paczynski 1967). The radiation emitted from this hydrogen-deficient class of objects should be detectable by instruments such as the Laser Interferometer Space Antenna (LISA), hence they are test-beds of gravitational wave physics (Kupfer et al. 2018). AM CVn stars are also of interest as a potential progenitor class of Type Ia supernovae (Brown et al. 2011; Gilfanov & Bogdán 2010; Shen & Bildsten 2014) and can offer important insights into binary evolution and common-envelope evolution.

Three channels of formation for AM CVn stars have been proposed. One possibility is via a double degenerate system that initially starts out as detached and then evolves to become interacting via mass transfer. However, this path has been in doubt since Shen (2015) found that it was vulnerable to mergers caused by classical-nova-like eruptions from the accreting white dwarf. Another channel is via a semi-degenerate helium (He) star channel, while a third is to evolve from a hydrogen-rich CV (see e.g. Nelemans et al. 2001a,b; Podsiadlowski, Han & Rappaport 2003; Yungelson 2008; Brooks et al. 2015). We currently face a conundrum in understanding the origin of helium-rich CVs because all identified pathways to their formation face problems when confronted with observations, for example the recent study of the eclipsing AM CVn, Gaia 14aae, (Green et al. 2019).

ES Ceti (ES Cet) was discovered by Noguchi, Maehara & Kondo (1980) and classified as a CV by Downes & Shara (1993). The optical magnitude range of the star is $16.5 - 16.8$, and with an absolute magnitude of $M_g = 5.6 \pm 0.4$, ES Cet is amongst the most luminous AM CVn stars (Ramsay et al. 2018). Warner & Woudt (2002) found a photometric period in optical photometry of ES Cet of 620 s. Photometric studies over a baseline of years showed the period to be highly coherent, albeit slowly increasing with time (Espaillat et al. 2005; Copperwheat et al. 2011; de Miguel et al. 2018). Combined with the helium-dominated emission line spectrum, it was natural to interpret the period as orbital. ES Cet has the third shortest orbital period currently known amongst AM CVn stars, after HM Cnc ($P_{orb} = 324$ s, Roelofs et al. 2010) and V407 Vul ($P_{orb} = 569$ s, Haberl & Motch 1995). ES Cet's period increases at a rate consistent with expectations for mass transfer driven by gravitational radiation (de Miguel et al. 2018). However, the orbital periods of both HM Cnc and V407 Vul decrease (Esposito et al. 2014 and references therein). This was shown to be possible if the donors in these stars still have significant surface hydrogen layers as a result of the prior evolution (D'Antona et al. 2006; Kaplan, Bildsten & Steinfadt 2012). There is indeed some evidence that hydrogen contributes to the emission line spectrum of HM Cnc (Roelofs et al. 2010). ES Cet may differ from these systems and is possibly more representative of the bulk of AM CVn stars.

Depending upon the size of the accretor in a mass-exchanging binary, it is possible that a disc is unable to form and instead the mass transferred ploughs directly into the accretor. This is familiar for main-sequence stars in the form of Algol binary stars. The same only becomes possible for typical white dwarfs at periods below ~ 10 min (e.g. Marsh & Steeghs 2002; Roelofs et al. 2010). Such direct impact is likely to lead to strong asymmetries visible in both photometry and spectroscopy. On the other hand if a disc forms, it tends to be relatively axisymmetric, albeit with a disturbance caused by the gas stream at the edge of the disc. In the case of discs we see broad absorption lines in some high-state systems or double-peaked line emission from the disc plus a feature associated with the gas

Table 1. Log of ES Cet observations.

Telescope	Date	Exp (sec)	UT interval	No. of frames
Magellan	27 Oct 2002	30 - 40	03:04 - 08:04	357
	28 Oct 2002	30 - 60	04:37 - 08:15	171
VLT	28 Oct 2003	60	00:03 - 08:23	230

stream/disc impact which executes a sinusoidal radial velocity curve with a full amplitude similar to the separation between the peaks (e.g. Marsh 1999; Morales-Rueda et al. 2003). HM Cnc and V407 Vul both appear to be in a state of direct impact (Barros et al. 2007). The next known AM CVn star, with a longer orbital period than ES Cet, SDSS J135154.46-064309.0 ($P_{orb} = 15.7$ min, Green et al. 2018) is disc-accreting system. ES Cet's period is close to the likely dividing line between direct impact and disc accretion and so its mode of accretion is not clear *ab initio*. Based on an analysis of the light curves, Espaillat et al. (2005) suggested that in fact ES Cet might be in a state of direct-impact accretion as well, but this issue has not been settled in the years since.

The issues outlined above motivated us to carry out a spectroscopic study of ES Cet. Spectroscopy moreover is a means to confirm the basic hypothesis that the 620 s photometric period is indeed the binary period. Likely though this seems, given the nature of ES Cet and the way in which its period is evolving, it should certainly be put to the test. The structure of this paper is the following: Section 2 contains details about observations. In Section 3 are described the average spectra. Section 4 presents information about the trailed spectra. Doppler maps are presented in Section 5. Study of polarisation and pulsations are reported in Section 6 and 7, respectively. The summary and conclusions of our campaign are in Section 8.

2. Observations

We acquired spectroscopy of ES Cet during two campaigns in 2002 and 2003. During the first run, 528 spectra were obtained on two nights from 2002 October 27 to 28. The Boller & Chivens Spectrograph (B&C) was used to acquire low-resolution spectra on the 6.5-m Magellan-Clay telescope at Las Campanas Observatory, and covered the range from 3850 to 5500 Å. A 0.7-arcsec slit and a 1200 line mm^{-1} grating yielded a spectral resolution of 2 pixels and a dispersion of $0.80 \text{ Å pixel}^{-1}$. A wide-slit exposure of the spectrophotometric standard star LTT377 was used to obtain a nominal count to flux calibration for the spectra.

The second run was conducted on 2003 October 28 using the FORS1 spectrograph on the VLT telescope. This time 230 spectra were obtained with the range from 4300 to 8600 Å. A 1.0-arcsec slit and a grism GRIS300V yielded a spectral resolution of 2 pixels and a dispersion of $5.30 \text{ Å pixel}^{-1}$ for 2x2 binning.

Table 1 gives an overview of our observations. All images were bias-subtracted and flat field-corrected. Extraction and calibration were carried out using the software packages PAMELA and MOLLY¹ (Marsh 1989).

3. Average spectra

The average Magellan and VLT spectra of ES Cet are shown on the left and right panels in Fig. 1, respectively. They con-

¹ <http://deneb.astro.warwick.ac.uk/phsaap/software/>

sist of a blue continuum with a series of strong emission lines. Most of the identifiable features can be interpreted as either neutral (HeI) or ionized (HeII) helium. The lines from neutral helium are weaker than the ionized helium peaks. Neither hydrogen nor metallic lines are detectable, apart from nitrogen. Nitrogen-rich matter is produced in the CNO-cycle, hence nitrogen seems to be abundant in most AM CVn stars (e.g. Marsh, Horne & Rosen 1991; Roelofs et al. 2009; Carter et al. 2014a; Kupfer et al. 2016).

To test for the presence of hydrogen in ES Cet, we plotted the 6560 Å line as a function of velocity two times over, first relative to the central wavelength corresponding to the HeII line, and second for H α line. We compare these to the velocity profile of HeII 4686 in Fig. 2. It is evident that the profiles are better aligned on the assumption that the 6560 line also comes from ionised helium rather than hydrogen. There is thus no evidence for hydrogen in ES Cet. We also measured the radial velocities of ES Cet from the HeII 4685.75 line, and from the wavelength corresponding to the 6560.10 HeII line and to the 6562.72 H α line. The mean difference between the 6560.10 – 4685.75 lines is -56.1 ± 1.8 km/s, while for the 6562.72 – 4685.75 case this would be 175.9 ± 1.8 km/s. Neither is consistent with zero (not surprising because there are some profile differences), but the HeII identification is clearly favoured.

Our measurements of line fluxes and equivalent widths are given in Table 2. The majority of these spectral lines have a broad, double-peaked profile, clearly seen in spectra of ES Cet, e.g. in the HeII 5411 line. This is a key feature of binary systems with accretion. In some AM CVn stars, triple-peaked emission lines are observed, i.e. GP Com (Marsh 1999), SDSS J120841.96+355025.2, SDSS J152509.57+360054.50 and SDSS J012940.05+384210.4 (Kupfer et al. 2013), SDSS J113732.32+405458.3, and SDSS J150551.58+065948.7 (Carter et al. 2014b). Smak (1975) and Nather, Robinson & Stover (1981) suggested that the lines are made up of a double-peaked profiles from an accretion disc, and a separate narrow component near the centre of the line known as a 'central spike'. This feature is thought to originate close to the surface of the accreting white dwarf (Marsh 1999; Morales-Rueda et al. 2003). There is no evidence for the 'central spike' feature in any of ES Cet's emission lines.

4. Trailed spectra

We present the phased-binned trailed spectra for the strongest HeII and HeI lines of ES Cet on the upper panels in Fig. 3 and Fig. 4. Twenty phase bins were equally spaced around the cycle and we have displayed one cycle repeated twice for clarity. The time-resolved spectra were folded on the ephemeris given by Copperwheat et al. (2011) (this spans the epochs of our spectra):

$$\text{BJD(TDB)} = 52200.980575(6) + 0.00717837598(3) E,$$

where E is the cycle number. The trailed spectra show clear evidence for double-peaked emission lines with a sinusoidal "S"-wave component superposed in most instances. Therefore, these data confirm that the 620 s photometric period is indeed orbital, beyond any doubt. To confirm this quantitatively, we measured radial velocities and computed the Lomb-Scargle periodogram corresponding to the strong HeII 4686 line (Fig. 6). A clear signal is seen at 139 cycles per day. A weaker group of peaks appears at 2 times this frequency. Zooming in on the main signal, one can see that the strongest peak occurs at $f = 139.306725$

cycles per day ($P_{\text{orb}} = 0.007178404$ days), with the two next-strongest peaks occurring at the usual ± 1 cycle per day aliases. The period of the strongest peak corresponds to the one presented by Copperwheat et al. (2011), and hence represents the orbital period of the binary.

In the upper panels of Figs 3 and 4, one can see a dark, near-horizontal line on the blue-shifted side of the HeII 4859, HeII 5411, HeII 4339 and HeII 4541 trailed spectra. HeII 4859 shows it best of all, and shows that it extends to the red-shifted side of the line, although bright-spot emission dominates on the red-shifted side beyond +400 km/s. The feature, which is shown magnified in Fig. 5 (indicated by the white lines), has all the signs of a "rotational disturbance" (Greenstein & Kraft 1959) caused as the disc is eclipsed by the mass donor. For instance, it occurs earliest in phase on the blue-shifted peak of the emission line, as expected for a prograde orbiting disc. The feature is seen close to phase zero on Copperwheat et al. (2011)'s ephemeris which is referenced to minimum light. This indicates that the photometric signal is primarily caused by eclipses of the disc. This association is further confirmed by the phasing of the S-wave which is in a standard location relative to phase zero in the trailed spectra, as also confirmed by the location of the bright emission in the Doppler maps.

Thus, we conclude that ES Cet's outer disc is eclipsed. The eclipse can be traced as far as ~ -800 km/s (Fig. 5). Given that the outermost velocity in the disc is around 600 km/s from the emission line peak velocity, and that $V \propto R^{-1/2}$ in a Keplerian disc, the eclipse therefore reaches a radius in the disc which is a fraction $(600/800)^2 \approx 50\%$ of the outer disc radius. The signal-to-noise ratio in the line wings prevents us from determining whether the eclipse reaches the white dwarf itself, although this seems unlikely given the 10 to 20% depth of the photometric eclipses (Copperwheat et al. 2011). Our spectra had exposure times of 60 s, corresponding to ~ 0.1 in terms of orbital phase, very comparable to the vertical extent of the eclipse feature in Fig. 5 at any one velocity in the lines. The data are therefore in effect vertically smeared by this amount, and so shorter exposure spectra have the potential to reveal deeper and sharper variations which may allow the orbital inclination of ES Cet to be pinned down. The eclipse may also encompass the bright spot, as is perhaps best indicated by the HeII 4859 trail in Fig. 5.

The various trails are similar, but not identical, and HeII 4686 in particular is noticeably asymmetric from red- to blue-shifted sides. The S-wave from the bright-spot also seems most visible at its extremes of radial velocity. These features may hint at vertical structure and self-obscurance within the disc. This may not be surprising as ES Cet is viewed at high inclination, and it is also a high accretion rate system.

5. Doppler maps

To accurately track the phase of the S-wave signal, we back-projected the trailed spectra into a Doppler tomogram (Marsh & Horne 1988). The method of Doppler tomography enables the projection of a series of phase-resolved spectra on to a two-dimensional map in velocity coordinates (for review: Steeghs 2003; Marsh 2001). In Doppler tomograms, emission features that are not stationary in the binary frame or move on a period different from the orbital period will spread out over the resulting Doppler tomogram, while stationary emission features add up constructively. Not only is the method of Doppler tomography useful to separate features that move with a different amplitudes and/or phase, but it allows tracking of asymmetric structures in accretion discs and reveals details of the gas flow in

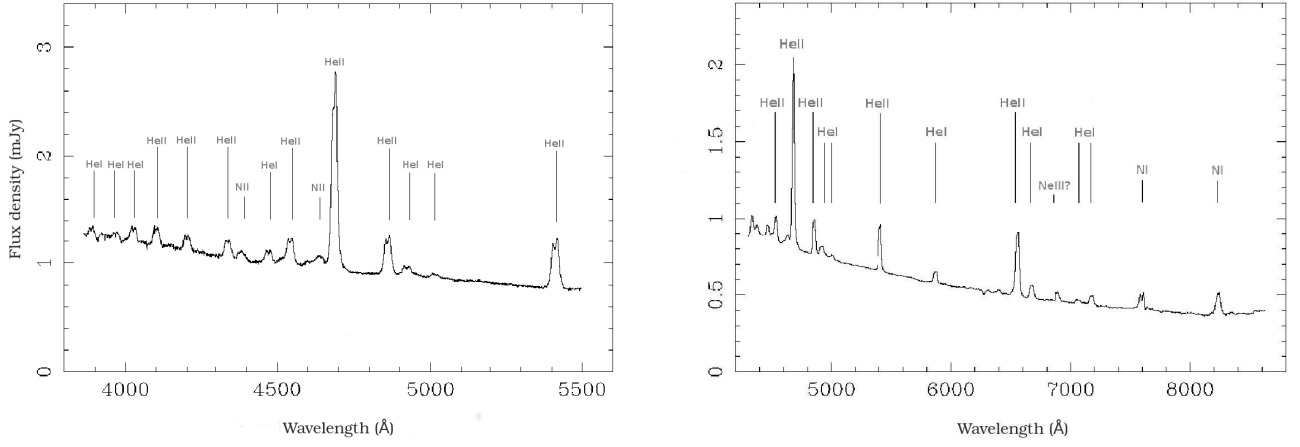


Fig. 1. The panels show the mean spectra of ES Cet taken with Magellan 27-28 Oct 2002 (left panel) and the VLT on 28 Oct 2003 (right panel). All lines can be identified with HeII, HeI and NII or NII.

Table 2. Mean fluxes and equivalent widths of lines of ES Cet.

Line	Magellan Flux $10^{-15} \text{ ergs s}^{-1}$	EW Å	Line	VLT Flux $10^{-15} \text{ ergs s}^{-1}$	EW Å
HeI 3888	2.6 ± 0.1	1.12 ± 0.05	HeII 4541	9.5 ± 0.2	6.50 ± 0.10
HeI 3964	3.8 ± 0.1	1.53 ± 0.05	HeII 4686	42.2 ± 0.2	38.2 ± 0.1
HeI 4026	5.7 ± 0.1	2.55 ± 0.05	HeII 4860	8.5 ± 0.1	8.74 ± 0.05
HeII 4100	6.7 ± 0.1	3.20 ± 0.05	HeI 4921	3.1 ± 0.1	3.32 ± 0.05
HeII 4200	5.1 ± 0.1	2.66 ± 0.05	HeI 5015	0.89 ± 0.1	1.01 ± 0.05
HeII 4339	6.6 ± 0.1	3.99 ± 0.05	HeII 5411	9.68 ± 0.1	14.4 ± 0.05
NII 4379	3.6 ± 0.1	2.25 ± 0.05	HeI 5876	2.2 ± 0.1	4.38 ± 0.05
HeI 4471	5.0 ± 0.1	3.37 ± 0.05	HeII 6560	50.1 ± 0.2	31.4 ± 0.1
HeII 4541	12.1 ± 0.2	8.51 ± 0.1	HeI 6678	2.3 ± 0.05	7.04 ± 0.1
NII 4643	7.0 ± 0.2	5.23 ± 0.1	NeIII 6886?	1.26 ± 0.05	4.32 ± 0.1
HeII 4686	55.1 ± 0.2	43.5 ± 0.1	HeI 7065	7.2 ± 0.2	2.7 ± 0.1
HeII 4860	11.7 ± 0.1	10.23 ± 0.05	HeI 7160	1.7 ± 0.2	6.89 ± 0.2
HeI 4921	3.4 ± 0.1	3.05 ± 0.05	NI 7608 ^a	-	-
HeI 5015	1.3 ± 0.1	1.25 ± 0.05	NI 8242	3.4 ± 0.2	20.74 ± 0.2
HeII 5411	13.0 ± 0.1	16.6 ± 0.1			

^a Line present but could not be measured reliably, due to a blend with another line.

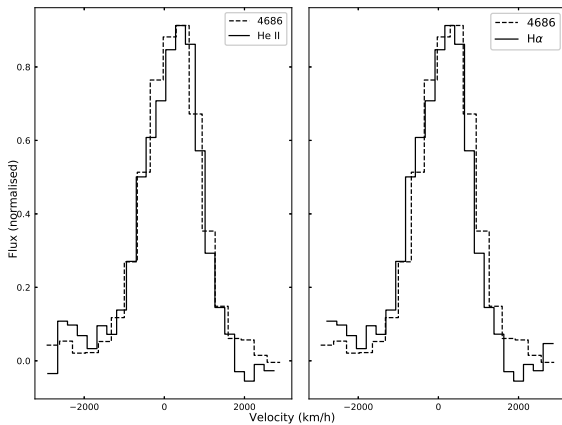


Fig. 2. The emission lines of ES Cet at 4686Å (dotted line) and 6560Å (black line). The 6560Å line was converted into velocity space treated as HeII line with a central wavelength of 6560.10Å (left panel), and as H α line with a central wavelength of 6562.72Å (right panel). Both lines are shifted but the discrepancy is more significant for H α case (see Sec.3).

a variety of systems. For analysis of AM CVn systems, Doppler tomography has also proved to be beneficial, e.g. for the investigation of the structure of an accretion disc (Breedt et al. 2012), the discovery of multiple bright spots (Roelofs et al. 2006a; Kupfer et al. 2013), or for searching for the presence of central spikes (Kupfer et al. 2016).

For all the trailed spectra, we computed the corresponding Doppler tomograms using the software package DOPPLER² (Marsh & Horne 1988). The tomograms are presented in the second rows of Fig. 3 and Fig. 4. The bottom panels show trailed spectra computed from the maps. Once again, for each map and trailed spectrum, we used the ephemeris given by Copperwheat et al. (2011). All the Doppler tomograms show a similar structure, with a bright ring corresponding to emission from the accretion disc. In the case of the bright spot, the situation is more complicated. It is located mostly towards the upper-left, which, as remarked above, is the expected location, but it has a smeared structure and is not consistent from line to line. Partly this might be azimuthal smearing due to ES Cet's short

² <https://github.com/trmrsh/trm-doppler>

period and the 60 s-long exposures as discussed earlier for the eclipses, but in addition, ES Ceti clearly is a very high accretion rate system, and the Doppler maps of high accretion rate CVs (nova-likes) have often proved hard to unravel, so we do not attach much significance to this finding. Indeed, compared to many nova-likes, which exhibit single-peaked lines even when deeply eclipsing, ES Ceti is well-behaved.

6. Polarimetry

Given the strong HeII emission in the magnetic polar (AM Her) class of CVs, we decided to obtain spectropolarimetry of ES Ceti. We took one night of circular spectropolarimetry using the FORS1 spectrograph of the VLT on 28 October 2003. We took spectra for slightly over 8 hours, obtaining 230 exposures of 60 seconds each, the remaining time taken up with overheads of rotating the Wollaston prism.

The average polarisation is consistent with zero, with an uncertainty of order 0.1 % (Fig. 7). To check that this could not be the result of cancellation of opposing senses of circular polarisation, we also calculated the power spectrum of the polarisation light curve integrated from 4400 to 7000 Å (Fig. 8). This is also a null result, and in this case we would have expected to detect a semi-amplitude of 0.05 %. We illustrate this by injection of such a signal at the expected frequency (dashed line in Fig. 8) which produces a peak of height ~ 6 , which has a probability (frequency known in advance) of $\exp(-6) \sim 0.25$ %. We conclude that there is no circular polarisation in ES Ceti at a level of 0.05 to 0.1 %, and thus no direct sign of magnetic accretion; the mystery of the absence of signs of magnetism amongst AM CVn stars continues.

7. Discussion

Several models have been proposed to explain the observed properties of the two shortest period AM CVn stars, HM Cnc and V407 Vul (Ramsay et al. 2000; Israel et al. 2003; Barros et al. 2007). The intermediate polar (IP) model (Motch et al. 1996) model holds that these systems are not ultra-compact binaries at all, but rather have orbital periods of several hours and the ultra-short periods then represent the spins of magnetic white dwarfs. The unipolar induction (UI) model (Wu et al. 2002) model is the only model without a Roche lobe filling secondary and is essentially equivalent to the model proposed by Goldreich & Lynden-Bell (1969) for the Jupiter–Io system. In the direct-impact accretion model (Marsh & Steeghs 2002) a Roche lobe-filling white dwarf loses its mass to its more massive white dwarf companion, and the accretion stream hits the accretor directly without forming a disc. This is presently the most widely-accepted model of HM Cnc and V407 Vul (Steeghs et al. 2006; Wood 2009; Roelofs et al. 2010). The natures of AM CVn stars with longer orbital periods, e.g. SDSS J135154.46-064309.0 ($P_{orb} = 15.7$ min, Green et al. 2018) and AM CVn itself ($P_{orb} = 17.1$ min, Nelemans, Steeghs & Groot 2001c), are better established. Their spectra show an absence of hydrogen, the presence of helium lines, many of which are the double-peaked emission (or absorption) lines characteristic of sources accreting via discs. Also, detection of one or even two bright spots are frequently reported (Kupfer et al. 2016). Based on the photometric observations, Espaillet et al. (2005) concluded that ES Ceti follows the direct-impact scenario and is therefore similar to HM Cnc and V407 Vul. However, we find instead clear evidence of an accretion disc along with a smeared

spot-like structure, placing it very much in the same bracket as the bulk of longer period AM CVn systems.

Although, ES Ceti has a disc and is more like the other ultra-compact binaries, AM CVn stars at longer periods than ES Ceti tend to have very different spectra with weak absorption lines, e.g. HP Lib (Roelofs et al. 2007). AM CVn itself (Roelofs et al. 2006b) shows an absorption spectrum dominated by HeI, with only HeII 4686 in emission whereas ES Ceti is very much an emission line system without any presence of absorption lines. This suggests a difference in the vertical temperature structure within the disc. That is, in AM CVn one sees light from a region where the temperature drops along the line of sight towards the observer, whereas in ES Ceti it increases. The high orbital inclination implied by the eclipses may also play a role. Support for this comes from Burdge et al. (2020)'s discovery of ZFT J1905+3134, an eclipsing AM CVn system with a period of ~ 17.2 minutes which also shows strong HeII emission features similar to ES Ceti.

8. Conclusions

We have described results of Magellan and VLT spectroscopic and spectropolarimetric surveys aimed at understanding the internal accretion structure of the helium-rich binary ES Ceti.

Time-resolved spectra reveal strong variability in the emission lines on the 620 s period found from photometry. Double-peaked emission is clearly visible in the lines in our spectra, as is characteristic of an accretion disc. This confirms that the photometric period of 620 s first reported by Warner & Woudt (2002) is ES Ceti's orbital period. We find no periodic signals on periods unrelated to the 620 s orbital period.

Due to the strong HeII emission in magnetic CVs, which is also seen in ES Ceti, we conducted one night of circular spectropolarimetry, but we found no circular polarisation placing an upper limit of 0.1 %. The strength of HeII in ES Ceti more likely reflects its high accretion rate and state of excitation.

We discovered a short-lived, phase-dependent flux deficit in the trailed spectra of the HeII 4859, HeII 5411, HeII 4339 and HeII 4541 lines, consistent with a "rotational disturbance" (Greenstein & Kraft 1959). This shows that the outermost parts of the disc in ES Ceti are eclipsed by the mass donor. The timing of the deficit is consistent with the phase of photometric minimum light, indicating that a significant part of the orbital light curve may be caused by eclipses. The eclipse extends over about half the outer disc in radius, but probably does not reach the white dwarf itself given the relatively shallow photometric eclipse. Higher time resolution spectroscopy of ES Ceti could refine the exact radial extent of the eclipse and therefore constrain the orbital inclination.

For all the trailed spectra, we computed the corresponding Doppler tomograms. All the Doppler tomograms show evidence for a similar structure, with a bright ring corresponding to emission from the accretion disk. Several also show a brightness maximum at the expected location of the gas stream / disc impact ("bright spot").

We conclude that, with the third shortest orbital period of any AM CVn star ($P_{orb} = 620$ s), ES Ceti is the system with the shortest orbital period that hosts an accretion disc, and that the disc is eclipsed.

Acknowledgements. Project was supported by Polish National Science Center grants awarded by decisions: DEC-2015/16/T/ST9/00174 for KB. TRM and DS acknowledge support from the Science and Technology Facilities Council (STFC) grant numbers ST/P000495/1 and ST/T000406/1. Based on observations

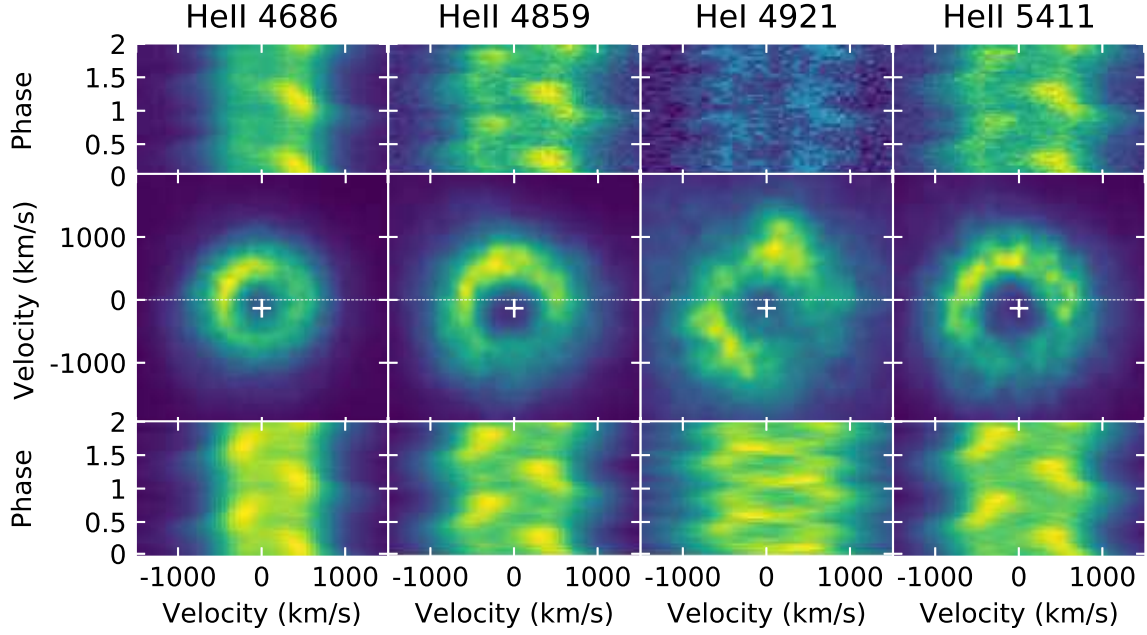


Fig. 3. The top panels show phase-folded, continuum-normalised and subtracted trailed spectra of four of the lines from the Magellan data. The middle and bottom panels show the equivalent Doppler maps and fits. White crosses mark the center of a disc. At phase 1, the HeII 4859 data show a dark feature, especially on the blue-shifted side, and slightly delayed in phase near zero velocity, that is the signature of an eclipse of the disc.

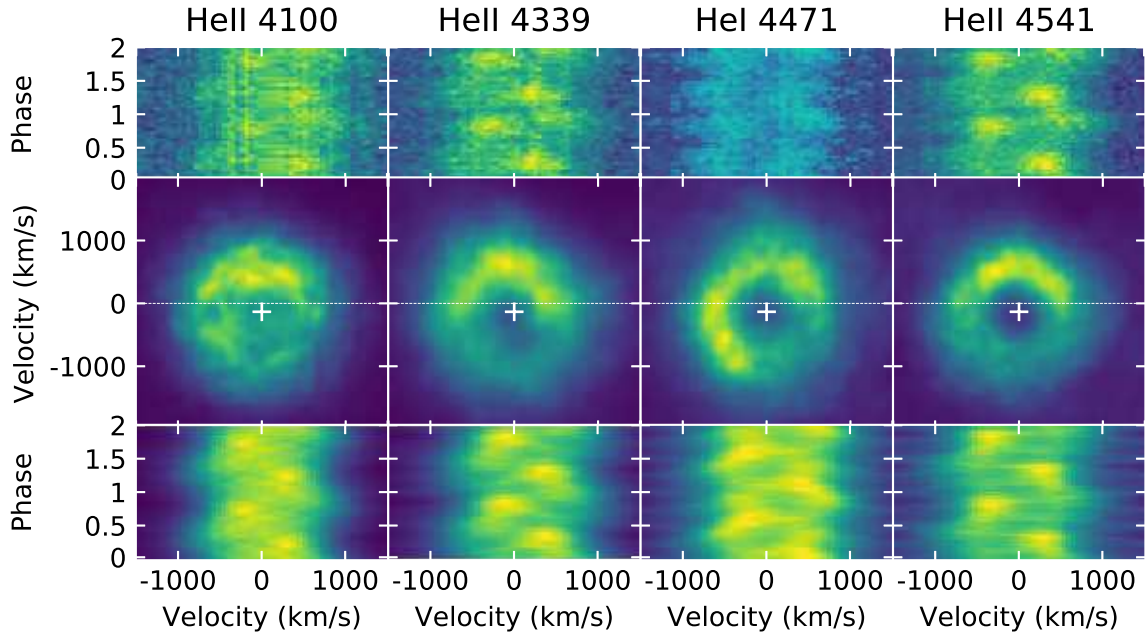


Fig. 4. As in Fig. 3, the trailed spectra and the equivalent Doppler maps and fits for four more lines from the the Magellan data.

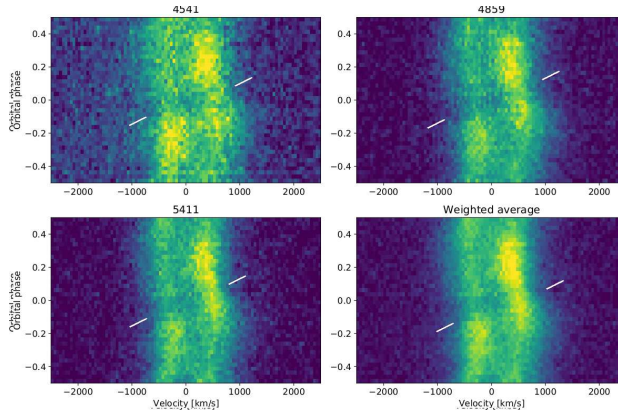


Fig. 5. The closeup of the profiles near eclipse in trailed spectra of three of the lines from the Magellan data: HeII 4541 (top left), HeII 4859 (top right), HeII 5411 (bottom left) and the average of these three lines (bottom right). The eclipse is indicated by the white lines and is visible as a darkening around phase 0.0 that slopes upwards from the blue- to

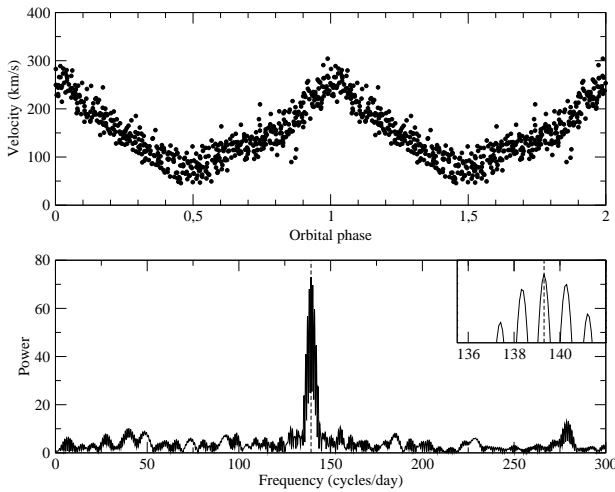


Fig. 6. Top panel shows the radial velocities of the disc through the "S"-wave measured from HeII 4686 line folded on the best fitting period. The bottom panel provides the Lomb-Scargle periodogram for the same line with a vertical dashed line showing the position of the Copperwheat's et al's ephemeris. A zoom presents a magnified view of the strongest peak.

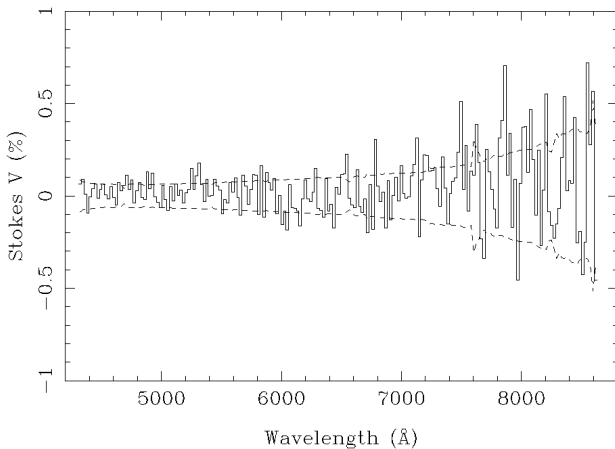


Fig. 7. The mean percentage circular polarisation of ES Ceti observed with the VLT on 28 October 2003. The dashed lines show the estimated uncertainties (1σ).

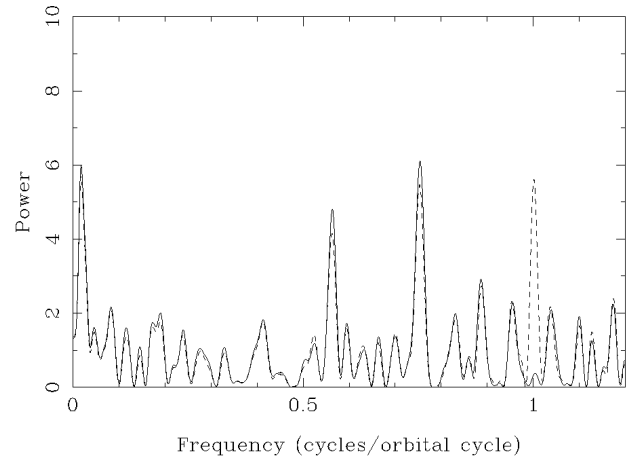


Fig. 8. The Lomb-Scargle periodogram of the light curve of the circular polarisation integrated from 4400 to 7000 Å. Any signal on the orbital period should appear at 1 cycle/orbital cycle. The dashed line shows the periodogram after the addition of a signal with a semi-amplitude polarisation of $\sim 0.05\%$ at the expected frequency.

collected at the European Organisation for Astronomical Research in the Southern Hemisphere under ESO programme 072.D-0119(A) as well as data gathered with the 6.5 meter Magellan Telescopes located at Las Campanas Observatory, Chile.

References

- Barros, S.C.C. et al., 2007, *MNRAS*, 374, 1334
 Breedt, E. et al., 2012, *MNRAS*, 425, 2548
 Brooks, J., Bildsten, L., Marchant, P., & Paxton, B., 2015, *ApJ*, 807, id. 78,
 Brown, W.R. et al., 2011, *ApJ Letters*, 737, id. L23
 Burdge, K.B. et al., 2020, arXiv:2009.02567
 Carter, P. J. et al., 2014a, *MNRAS*, 437, 2894
 Carter, P. J. et al., 2014b, *MNRAS*, 439, 2848
 Copperwheat, C. M. et al., 2011, *MNRAS*, 413, 3068
 D'Antona, F., Ventura, P., Burderi, L. & Teodorescu, A., 2006, *ApJ*, 653, 1429
 de Miguel, E. et al., 2018, *ApJ*, 852
 Downes, R.A. & Shara, M.M., 1993, *PASP*, 105, 127
 Espaillat, C. et al., 2005, *PASP*, 117, 189
 Esposito, P., Israel, G. L., Dall'Osso, S. & Covino, S., 2014, *A&A*, 561, id. A117
 Green, M. J. et al., 2018, *MNRAS*, 477, 5646
 Green, M. J. et al., 2019, *MNRAS*, 485, 1947
 Greenstein, J. L. & Kraft, R. P., *ApJ*, 130, 99
 Gilfanov, M. & Bogdán, Á., 2010, *Nature*, 463, 924
 Goldreich, P. & Lynden-Bell, D., 1969, *ApJ*, 156, 59
 Haberl, F. & Motch, C., 1995, *A&A*, 297, L37
 Israel, G. L. et al., 2003, *ApJ*, 598, 492
 Kaplan, D. L., Bildsten, L. & Steinfeldt, J. D. R., 2012, *ApJ*, 758, id. 64
 Kupfer, T. et al., 2013, *MNRAS*, 432, 2048
 Kupfer, T. et al., 2016, *MNRAS*, 457, 1828
 Kupfer, T. et al., 2018, *MNRAS*, 480, 302
 Marsh, T.R., 1989, *PASP*, 101, 1032
 Marsh, T.R., 1999, *MNRAS*, 304, 443
 Marsh, T.R. & Horne, K., 1988, *MNRAS*, 235, 269
 Marsh, T.R., Horne, K. & Rosen, S. 1991, *ApJ*, 366, 535
 Marsh, T.R., 2001, in Boffin, H.M.J., Steeghs, D. & Cuypers, J., eds, *Lecture Notes in Physics*, Springer Verlag, Berlin, 573, 1
 Marsh, T.R. & Steeghs, D., 2002, *MNRAS*, 331, L7
 Marsh, T.R., Nelemans, G. & Steeghs, D., 2004, *MNRAS*, 350, 113
 Morales-Rueda, L. et al., 2003, *A&A*, 405, 249
 Motch, C. et al., 1996, *A&A*, 307, 459
 Nather, R. E., Robinson, E., L., & Stover, R., J., 1981, *ApJ*, 244, 269
 Nelemans, G. et al., 2001a, *A&A*, 365, 491
 Nelemans, G. et al., 2001b, *A&A*, 368, 939
 Nelemans, G., Steeghs, D., & Groot, P. J., 2001c, *MNRAS*, 326, 621
 Noguchi, T., Maehara, H. & Kondo, M., 1980, *Tokyo Astronomical Observatory, Annals*, 18, 55
 Paczyński, 1967, *Acta Astron.*, 17, 287
 Pala, A. F. et al., 2020, *MNRAS*, 494, 3799
 Podsiadlowski, P., Han, Z., & Rappaport, S., 2003, *MNRAS*, 340, 1214

Ramsay G., Cropper M., Wu K., Mason K. O. & Hakala P., 2000, MNRAS, 311,

75

Ramsay, G. et al., 2018, A&A, 620, A141

Roelofs, G.H.A. et al., 2006a, MNRAS, 365, 1109

Roelofs, G.H.A. et al., 2006b, MNRAS, 371, 1231

Roelofs, G.H.A. et al., 2007, MNRAS, 379, 176

Roelofs, G.H.A. et al., 2009, MNRAS, 394, 367

Roelofs, G.H.A. et al., 2010, ApJ Letters, 711, L138

Shen, K. J. & Bildsten, L., 2014, ApJ, 785, id. 61

Shen, K. J., 2015, ApJ, 805, id. L6

Smak, J., 1967, Acta Astron., 17, 255

Smak, J., 1975, Acta Astron., 25, 227

Solheim, J.-E., 2010, PASP, 122, 1133

Steehgs, D., 2003, MNRAS, 344, 448

Steehgs, D. et al., 2006, ApJ, 649, 382

Warner, B., 1995, Cataclysmic Variable Stars, Cambridge Univ. Press, Cambridge

Warner, B. & Woudt, P.A., 2002, PASP, 114, 129

Wood, M.A., 2009, MNRAS, 395, 378

Wu, K. et al., 2002, MNRAS, 331, 221

Yungelson, L. R., Astronomy Letters, 34, 620